

6.2 DATA ASSIMILATION WITH AN UNSTABLE SHALLOW WATER SYSTEM USING CYCLING REPRESENTER ALGORITHMS

Liang Xu* and Roger Daley
Naval Research Laboratory,
7 Grace Hopper Ave., Monterey, CA 93943-5502

1. INTRODUCTION

Operational meteorological centers around the world are either implementing or developing advanced four-dimensional data assimilation systems. With respect to the present operational three-dimensional variational (3DVAR) data assimilation algorithms, the advanced four-dimensional systems have several advantages. First, the observations are assimilated at the correct observation times, rather than being time-binned in the intermittent 3DVAR systems. Second, it is possible to properly account for serial correlations in the observations. Third, and perhaps most significantly, the all-important background error covariances can become, at least partially, flow-dependent.

The advanced four-dimensional algorithms fall into two classes. The first class contains sequential algorithms based on the Kalman filter and contains many variants such as the ensemble Kalman filter, extended Kalman filter, Kalman smoother etc. The second class contains the variational algorithms, which are all approximations to the generalized inverse problem. In the variational algorithms, one seeks to minimize a four-dimensional cost function, which measures the fit to the initial conditions, the observations, the model and spatial boundary conditions. In strong-constraint minimization, the prediction model is assumed to be perfect, thus eliminating one term from the cost function. In the more sophisticated (and expensive) weak constraint algorithms, one does not make the perfect model assumption.

As for the 3DVAR algorithms, the four-dimensional variational algorithms can be posed in one of two different spaces – model space and observation space. Traditionally, model space has been the preferred choice for atmospheric four-dimensional variational algorithms, but there exists a complete theory for four-dimensional variational assimilation in observation space. This theory is known as representer theory and has been extensively developed and applied to oceanographic data assimilation problems by Bennett (1990).

The oceanographic representer algorithms generally perform minimizations over a single (long) time-period to provide state estimates and derived quantities, leading

to increased understanding of ocean circulations. Conversely, data assimilation in the atmosphere is concerned with providing initial state estimates for prediction models to estimate future atmospheric states. Thus, in atmospheric data assimilation, most operational centers operate data assimilation cycles in near real time. Consequently, Xu and Daley (2000) extended the representer theory to produce the *cycling representer algorithm*.

In all four-dimensional variational data assimilation algorithms, the user must specify the initial and observation error covariances, the model error covariance (in the weak case) and perhaps boundary error covariances. The success of the data assimilation depends critically on the accurate specification of these covariances. For oceanographic data assimilation, where the minimization period is long, the initial error covariances only influence the early part of the period and have little influence over most of the period. Thus, for oceanographic problems the specification of the initial error covariances is not very critical. In atmospheric data assimilation, where the assimilation cycles are very short (3-12 hours), the specification of the error covariance at the beginning of each cycle is very important.

The cycling representer data assimilation algorithm of Xu and Daley (2000) is a weak constraint four-dimensional variational data assimilation algorithm, which provides an internally consistent estimate of the error covariance at the beginning of each cycle, based on the results of the previous cycle (and implicitly all previous cycles). In Xu and Daley (2000), the cycling representer algorithm was applied to a one-dimensional transport problem and was able to successfully extract the signal from noisy and sparse observations. However, the algorithm is very computationally demanding and awaits considerable enhancement in computer power before being practical for operational forecast models.

Because of the computational expense of the cycling representer algorithm of Xu and Daley (2000), an accelerated form has been developed (Xu and Daley, 2001). In the accelerated cycling representer algorithm, the representer matrix is calculated implicitly and the initial background error covariance at the beginning of each cycle is specified rather than being calculated. This is much more computationally tractable than the cycling representer algorithm itself and could be implemented for operational models on the computers of today.

* Corresponding author address: Liang Xu, Naval Research Laboratory, Monterey, 7 Grace Hopper Ave., CA 93943, USA; email: xu@nrlmry.navy.mil

We have two objectives in this paper. The first objective is to apply the cycling representer algorithm to a more realistic and computationally demanding data assimilation problem than the study of Xu and Daley (2000). Specifically, the problem is a two-dimensional, multivariate barotropically unstable shallow water system. The second objective is to apply the *accelerated cycling representer algorithm* of Xu and Daley (2001) to the same problem. The results are also compared with the ones using the *original representer algorithm* of Bennett (1990).

2. THE DATA ASSIMILATION SYSTEM

The data assimilation system used in this study consists of three components. They are the data assimilation algorithms, the prediction and the adjoint models of a linear shallow water equation system, respectively. Three different representer algorithms were used in this study. They are the original representer algorithm (Bennett, 1990), the cycling representer algorithm (Xu and Daley, 2000), and the accelerated cycling representer algorithm (Xu and Daley, 2001).

The shallow water system is one of the simplest and most frequently used test beds for applications in meteorology. Despite the overall simplicity of the system, it displays some of the complex multivariate, multidimensional interactions that are commonly observed in more comprehensive meteorological systems, such as the primitive equation system. A shallow water version of the Coupled Ocean /Atmosphere Mesoscale Prediction System (COAMPS) was used to construct the numerical tangent linear and adjoint models. Readers who are interested in the numerical techniques used in COAMPS can find detailed descriptions in Xu (1995) or Hodur (1997). The model domain consisted of a rectangle of 3850 km by 3850 km. There were 11 gridpoints in east-west (x-) and north-south (y-) directions, respectively. The total assimilation time period was 96 hours with a timestep of 600 s.

3. THE DATA ASSIMILATION EXPERIMENTS

In this study, we conducted 3 experiments, namely cycling with covariance updating (cycling representer), cycling with no covariance updating (accelerated cycling representer) and non-cycling (standard representer), respectively.

A basic state cosine-square jet similar to the one of Todling and Ghil (1994) was used to generate the needed barotropic instability. Singular vector analysis was employed to explicitly obtain all the singular vectors associated with the unstable system. The "true" solution for the problem was not chosen to be the leading unstable mode, but rather, was a "neutral" mode. We felt that this choice would be a particular tough test of any data assimilation system, because any discrepancies or faults of the data assimilation system

could easily excite an unstable mode and the error would grow rapidly.

Almost perfect observations were created from the "true" solution. We used a special observation network. In it, observations collocated with the 11 model gridpoints were available for the geopotential and wind components every 6 hours along a fixed line in the north-south direction ($x = 5$), as indicated by the black lines in Figure 1. This network had a maximum spatial coverage in the y-direction at $x = 5$ as indicated in Figure 2, but with a very poor coverage in the x-direction. We had 11 observations available along the line of $x = 5$ twice in each 12-hour short cycle for the cycling experiments and 16 times in the single long cycle for the non-cycling experiment, respectively. This network was created to see if the data assimilation systems were capable of spreading the sparse information as we hoped.

The initial ($t = 0$) background conditions were always specified to be everywhere equal to zero for the non-cycling experiments. For the cycling experiments, only the initial background conditions for the first cycle were specified equal to zero, the initial background conditions for the subsequent cycles were actually provided by the analysis at the end of the previous cycle.

We arbitrarily specified homogeneous, diagonal, univariate initial ($t = 0$) background error covariances for the geopotential and wind components. We know from experience that such error covariances are, in actuality, far from diagonal and are often multivariately-coupled, but we wished to make the initial error covariances simple and not very realistic.

4. THE RESULTS

We first demonstrate the performance of the three representer algorithms at hour 96 using the special observation network, by displaying in Figure 1, the wind and geopotential analyses and comparing them to the "true" solution. The geopotential fields are in grayscale (see thermometer on the right) while the wind fields are plotted as streamlines. Figure 1 (a) is the evolution of the "neutral" mode at hour 96 and is used as the "true" solution. The wind and geopotential analyses produced by the cycling, accelerated cycling, and non-cycling representer algorithms are displayed in Figure 1 (b), (c) and (d), respectively. All three algorithms appeared to be capable of capturing the main features of the "true" solution at the end of 96 hours as indicated in Figure 1. Among the three algorithms, the cycling representer appeared to be the most accurate and closest to the "true" solution (comparing panels (a) and (b)). The results from both the accelerated cycling (panel (c)) and the non-cycling representer (Panel (d)) algorithms were less accurate than from the cycling representer algorithm. Panels (c) and (d) have some similarity, particularly the distortions near the left boundaries in the x-direction. We attribute these distortions to the misspecification of the initial background error covariance.

(As noted earlier, in the non-cycling algorithm the poor initial error covariance is only prescribed at $t = 0$, while for the accelerated cycling representer, it is prescribed at the beginning of every cycle).

To further compare the overall accuracies of the analyses during the whole period of data assimilation, we used the square root of total perturbation energy (SRTPE) as an indicator to represent the overall error at any given timestep. Figure 2 displays the plots of SRTPE against time for the three different assimilation algorithms. The dotted line represents the results from the non-cycling algorithm. The long-dash dotted line represents the accelerated cycling representer algorithm (no covariance updates). The solid line represents the cycling representer algorithm (covariance updated every cycle). All three algorithms produced stable analyses, despite the model being barotropically unstable.

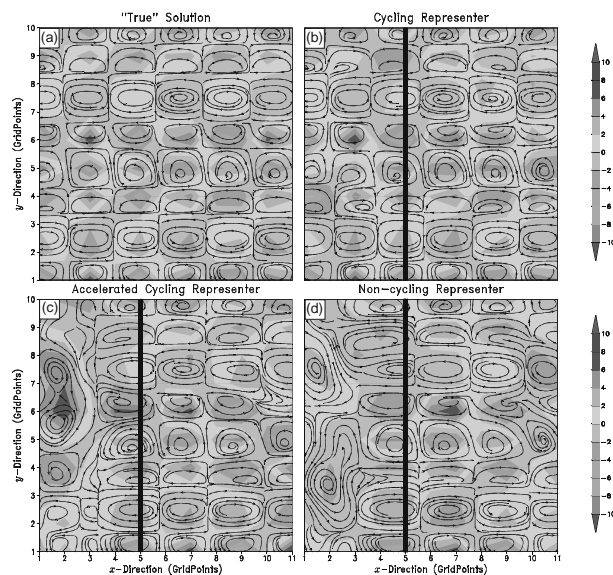


Figure 1. The wind fields (streamlines) and the geopotential fields (in grayscale) at hour 96 (end of the data assimilation period) from the “true” solution and three different representer algorithms. Panels (a), (b), (c), and (d) show the “true”, the cycling representer, the accelerated cycling representer, and the non-cycling representer solutions, respectively.

The cycling representer algorithm (solid line) indicated a steady reduction of overall errors measured by the SRTPE metric. The error levels were essentially flat during each cycle and the error reduction occurred at the end of each cycle (rather reminiscent of the behavior of a Kalman filter). The accelerated cycling representer algorithm (long dashed line) also showed a steady reduction of the overall errors measured by the SRTPE metric. The accelerated cycling and the cycling representer algorithms gave exactly the same results in the first cycle, but in later cycles, the covariance update of the cycling representer is clearly advantageous. It is unfortunate that covariance updating is so computationally burdensome.

The non-cycling algorithm (dotted line) was superior in the first 24 hours, which is to be expected, because it attempts to find the best fit over the whole 96-hour period. In the non-cycling representer algorithm, all the observations are inserted in one period and have about the same influence on the analysis. This is different from the cycling representer algorithms where the earlier observations influence the later analyses, but later observations do not influence earlier analyses.

From computational a point of view, the accelerated cycling representer algorithm was the most inexpensive one, followed by the non-cycling representer algorithm. The cycling representer algorithm was the most expensive. From an accuracy point of view, the cycling representer algorithm produced the most accurate overall analyses overall, followed by the non-cycling representer algorithm. However, the accelerated cycling representer algorithm was more accurate at the end of the period (hour 96) than the non-cycling algorithm and the error level was still decreasing.

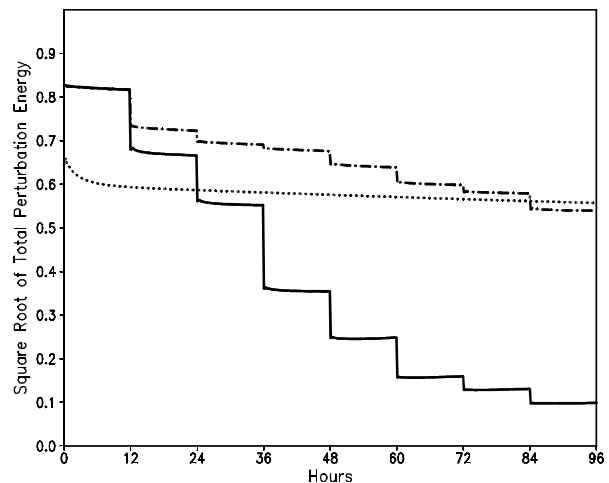


Figure 2. The overall error level (from the SRTPE metric, equation 12) as a function of time (in hours) for three different algorithms, using observation Network A. The solid, long-dashed, and dotted lines are for the cycling, accelerated cycling, and non-cycling representer algorithms, respectively.

5. SUMMARY AND CONCLUSIONS

A linear shallow water version of COAMPS with a barotropically unstable basic state was used as the test bed to conduct three advanced data assimilation experiments. The barotropic instability was produced through the use of a cosine-square jet profile in the basic state. The system had a sufficiently small number of degrees of freedom that all of the singular values and vectors of this system over a 96-hour time interval could be obtained explicitly. A “neutral” eastward-propagating mode was selected as the initial condition for a model integration to obtain the “truth”, against which all data assimilation experiments were to be evaluated.

Almost perfect observations for a special observation network was obtained by sampling the “true” solution. For the network three data assimilation algorithms were tested. First, there was the cycling representer algorithm (which includes error covariance update at the beginning of each cycle). The second algorithm was the accelerated cycling representer algorithm (which is much less computationally-intensive and does not update error covariances). The final algorithm was the non-cycling (single long cycle) representer algorithm.

All three representer algorithms were found to produce stable results for the network, despite the possibility of enormous error growth associated with the dynamically unstable system. The cycling representer algorithm (which updates error covariances at the beginning of each cycle) produced the most accurate analysis at the end of the data assimilation period. The non-cycling algorithm provided the most accurate state estimate at the beginning of the data assimilation period, but the worst state estimate at the end. By using a single long cycle, the non-cycling algorithm provided a “uniform” fit (similar error reduction) throughout the assimilation period. The accelerated cycling representer produced the same result as the cycling representer algorithm in the first cycle, but it had slower error reductions for subsequent cycles. This was not surprising, because we had deliberately chosen a rather poor representation of the error covariance to be specified at the beginning of each cycle.

The results from the accelerated representer algorithm were very encouraging because it is sufficiently computationally-tractable to be used on present day multi-processor machines for operational applications. It is clear from our experiments, that the assimilation errors were steadily reduced after each cycle for this algorithm, although the poor specification of error covariance at the beginning of each cycle led to less error reduction than would have been desirable. It is likely that a more realistic initial error covariance based on the statistical approaches used in 3DVAR algorithms would be helpful. Beyond that, there is always the possibility of using ensemble techniques to introduce more flow-dependence into the initial error covariances.

An effort at the Naval Research Laboratory (NRL) in Monterey is currently underway to construct a four-dimensional variational global data assimilation system using the accelerated cycling representer algorithm. This algorithm is being constructed for massively parallel machines and involves the parallel tangent linear and adjoint models of NOGAPS (Navy Operational Global Atmospheric Prediction System – Hogan and Rosmond, 1991). The observation and forward instrument modeling, as well as the construction of the initial error covariances, all comes from NAVDAS (NRL Atmospheric Variational Data Assimilation System – Daley and Barker, 2000, 2001). This new algorithm, which we refer to as NAVDAS A/R (for NAVDAS accelerated representer), is a natural extension of the

three-dimensional observation space NAVDAS system to four dimensions.

6. ACKNOWLEDGEMENTS

The authors would like to thank Carolyn Reynolds of NRL in Monterey for discussions regarding various aspects of singular vector analysis. We would also like to thank Andrew Bennett of FNMOC and Boon Chua of Oregon State University for discussions and assistance during this project. Support of the sponsor, NRL under Program Element 0601153N is gratefully acknowledged.

7. REFERENCES

- Bennett, A. F. 1990: Inverse methods for assessing ship-of-opportunity networks and estimating circulation and winds from tropical expendable bathythermograph data. *J. Geophys. Res.*, **95**, 16111-16148.
- Daley, R. and E. Barker, 2000: The NAVDAS Source Book, Defense Printing Office for the *Naval Research Laboratory*, 217 pp.
- Daley, R. and E. Barker, 2001: NAVDAS – formulation and diagnostics. *Mon. Wea. Rev.*, **129**, 869-883.
- Hodur, M. R., 1997: The Naval Research Laboratory's coupled ocean/atmosphere mesoscale prediction system (COAMPS). *Mon. Wea. Rev.*, **125**, 1414-1430.
- Hogan, T., and T. Rosmond, 1991: The description of the Navy Operational Global Atmospheric Prediction System's spectral forecast system. *Mon. Wea. Rev.*, **119**, 1786-1815.
- Todling, R. and M. Ghil, 1994: Tracking atmospheric instabilities with the Kalman filter. Part I: Methodology and one-layer results. *Mon. Wea. Rev.*, **122**, 183-204.
- Xu, L. and R. Daley, 2001: Data assimilation with a barotropically unstable shallow water system using representer algorithms. (In preparation)
- Xu, L. and R. Daley, 2000: Towards a true four-dimensional data assimilation algorithm: Application of a cycling representer algorithm to a simple transport problem. *Tellus*, **52A**, 109-128.
- Xu, L., 1995: The study of mesoscale land-air-sea interaction processes using a nonhydrostatic model. Ph.D. dissertation, *North Carolina State University, Raleigh*, 336 pp. [Available from Department of Marine, Earth and Atmospheric Sciences, North Carolina State University, Raleigh, NC 27695]